

Iskra, *ibid.* **3**, 2939 (1961) [*ibid.* **3**, 2148 (1962)].

²⁴H. Fröhlich and B. V. Paranjape, Proc. Phys. Soc. (London) **B69**, 21 (1956).

²⁵I. M. Dykman and P. M. Tomchuk, Fiz. Tverd. Tela **2**, 2228 (1960) [Soviet Phys. Solid State **2**, 1988 (1961)].

²⁶G. B. Benedek, W. Paul, and H. Brooks, Phys. Rev. **100**, 1129 (1955).

²⁷S. M. de Veer and H. J. G. Meyer, in *Proceedings of the International Conference on the Physics of Semiconductors, Exeter* (The Institute of Physics and the Physical Society, London, 1962), p. 358.

²⁸N. I. Meyer and M. H. Jørgensen, J. Phys. Chem. Solids **20**, 823 (1965).

²⁹E. G. S. Paige (private communication).

³⁰K. Seeger and D. Schweizer, J. Phys. Soc. Japan Suppl. **21**, 415 (1966).

³¹M. I. Nathan, W. Paul, and H. Brooks, Phys. Rev. **124**, 391 (1961).

³²R. A. Smith, *Semiconductors* (Cambridge U. P., Cambridge, England, 1964).

³³M. Glicksman, Phys. Rev. **105**, 865 (1957).

³⁴E. M. Conwell, Phys. Rev. **135**, A1138 (1964).

Spectroscopic Study of the Deformation-Potential Constants of Group-III Acceptors in Germanium[†]

R. L. Jones* and P. Fisher

Department of Physics, Purdue University, Lafayette, Indiana 47907

(Received 27 February 1970)

The effect of uniaxial compression on the excitation spectra of group-III impurities in germanium is presented and discussed. The deformation-potential constants b' and d' for the ground states are deduced on the basis of the piezospectroscopic effects for the C and D lines. Although there is a slight chemical-species dependence of b' and d' , the average values of these are -1.4 and -2.5 eV, respectively. These, in turn, lead to the values of -2.5 and -4.1 eV for b and d , the corresponding parameters for the valence band, using the relationships given by Bir *et al.* The values of b and d thus calculated agree in sign and magnitude with those determined by other methods. This is in contrast to the results obtained on the basis of the previous interpretation, in which the final state of the B line is assumed to have Γ_7 symmetry.

I. INTRODUCTION

A study of the electronic excitation spectra of impurities in semiconductors under uniaxial strain provides direct information about the deformation-potential constants of the energy states of the impurity. In the case of group-V impurities in germanium or silicon, the stress-induced splittings of the excited p states are the same¹⁻³ as those of the conduction-band minima; hence the corresponding deformation-potential constant of the host can also be readily obtained from the piezospectroscopy of the impurities. For the shallow donors, the dependence of the ground states on the applied force is relatively simple and well understood.¹⁻³ Because of the complexity of the top of the valence bands of silicon and germanium, the effective-mass description of the shallow acceptor impurities⁴⁻⁶ in these materials is considerably more complicated than for the group-V donors.⁴ The effective-mass wave equation for acceptors consists of a set of coupled differential equations, each involving all

valence-band edges. Thus, under the effect of a uniaxial force, the sublevels of an excited impurity state do not follow a given band edge in a simple manner, as is the case for the group-V impurities. In fact, as discussed by Bir *et al.*⁷ and Suzuki *et al.*,⁸ an explicit relationship between the splitting of the ground state of a group-III acceptor and that of the valence-band edge can only be obtained from a detailed knowledge of the wave functions of the impurity state. These authors have used the effective-mass wave functions for this purpose. Given the deformation-potential constants of the impurity state, such an approximation should be sufficient to predict the correct sign of the valence-band deformation-potential constants, if not the magnitude.

The first piezospectroscopic study of a group-III impurity in silicon or germanium was that of Jones and Fisher for thallium in germanium.⁹ More recently, a study was made of group-III impurities in germanium by Dickey and Dimmock¹⁰ and group-III impurities in silicon by Onton *et al.*¹¹ The inter-

pretation of the piezospectroscopic effects for group-III impurities in germanium assumed⁹ that the *B* line was due to a transition to a twofold-degenerate excited state.¹² This assumption was also used by Dickey and Dimmock, who, on this basis, deduced deformation-potential constants for the valence-band edge; they found these to be different in both sign and magnitude from those obtained by other methods. The purpose of the present paper is to present further spectroscopic data for the case of group-III impurities in germanium and to consider a new interpretation which predicts deformation-potential constants that agree in both sign and magnitude with those otherwise obtained.

II. EXPERIMENTAL PROCEDURE

The germanium samples studied were cut from thallium-doped single-crystal ingots with $\langle 110 \rangle$ growth axes; in the present measurements thallium was the only group-III impurity whose spectrum was examined. The ingots were oriented either by x rays or by the optical method described by Hancock and Edelman.¹³ In the wavelength region of interest, optical surfaces formed by grinding successively with Nos. 600, 1200, and 3200 carborundum and then etched to a "highly reflective" surface were found to be satisfactory. A single-beam single-pass Perkin-Elmer grating monochromator, model 98-G, was used for the measurements, and was calibrated using the pure rotational absorption spectra of atmospheric water vapor.¹⁴ An Eppley Golay system was used as detector. A glass optical cryostat¹⁵ was employed to cool the samples to temperatures near that of liquid helium. Both this and the Golay detector were equipped with optical windows of crystalline quartz, suitably wedged to suppress channeled spectra. The cryostat windows had a 1° wedge, each being cut so that the optic axis was essentially normal to the surface.

The samples were compressed uniaxially following a differential thermal contraction technique similar to that described by Rose-Innes.^{16,17} From a comparison with the results obtained for arsenic impurity in germanium,¹⁸ using the same compression arrangement, it is estimated that the maximum strain achieved was about 10^{-4} , which corresponds to a stress of about 10^8 dyn/cm². The spectra obtained under compression were studied using polarized radiation. The far-infrared radiation was polarized using a "pile-of-plates" polyethylene polarizer.¹⁹ It should be noted that crystalline quartz, one of the classic optically active materials for visible light, has an optical rotation of less than 2° per mm at a wavelength of 88μ ; thus, the 1-mm-thick quartz entrance window on the cryostat should not significantly affect the

plane of polarization of the light. The data obtained were processed by the method described by Onton *et al.*¹¹

III. THEORY

The theory of acceptor states associated with group-III impurities in germanium or silicon has been summarized by Dickey and Dimmock,¹⁰ Onton *et al.*,¹¹ and Fisher and Ramdas.³ The ground-state wave functions of the acceptor form a basis for the irreducible representation Γ_8 of the double group \bar{T}_d ,²⁰ while the excited-state wave functions form a basis for either Γ_6 , Γ_7 , or Γ_8 . A calculation of the energies of the impurity states was made by Mendelson and James⁶ for the case of germanium. A comparison of the results of this calculation with the experimental excitation spectra was given by Jones and Fisher¹²; this correlation is presented in Fig. 1.

The behavior under stress of the impurity states and those of the valence-band edge to which they are related has been considered explicitly by Pikus and Bir,²¹ Kleiner and Roth,²² Bir *et al.*,⁷ and Suzuki *et al.*⁸ A general description of the behavior of states with these symmetries has been given by Kaplyanskii.²³ The notation of Bir *et al.*⁷ will be used here. In the effective-mass approximation, the fourfold-degenerate Γ_8 ground state of the impurity is characterized by an angular momentum $J = \frac{3}{2}$. Under an applied uniaxial force \bar{F} the m_J

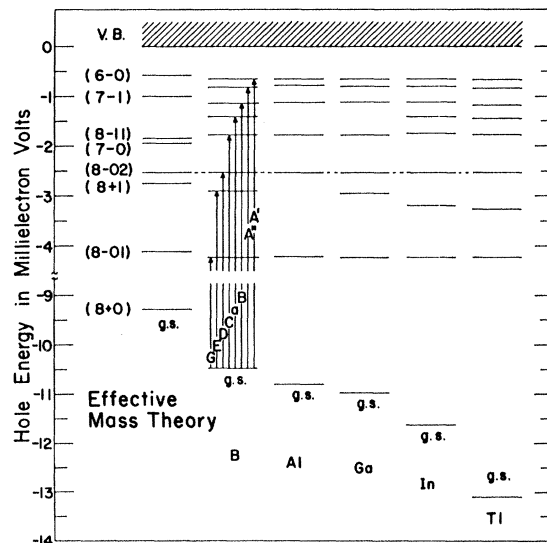


FIG. 1. Correlation of experimental and theoretical energy-level schemes of group-III acceptors in germanium. The final state of the *D* transition has been assumed to be the (8-02) effective-mass state as is implied by the short dashed lines connecting these states (see Ref. 12). V. B. designates the valence band.

$= \pm \frac{3}{2}$ states separate from the $m_J = \pm \frac{1}{2}$ states for $\vec{F} \parallel \langle 100 \rangle$ and $\vec{F} \parallel \langle 111 \rangle$. The extent of the splitting is given by

$$E_{\pm 3/2} = +\frac{1}{2} \Delta'_{100}, \quad (1)$$

$$E_{\pm 1/2} = -\frac{1}{2} \Delta'_{100}, \quad \text{for } \vec{F} \parallel \langle 100 \rangle,$$

where $\Delta'_{100} = 2b'(s_{11} - s_{12})T$, and

$$E_{\pm 3/2} = +\frac{1}{2} \Delta'_{111}, \quad (2)$$

$$E_{\pm 1/2} = -\frac{1}{2} \Delta'_{111}, \quad \text{for } \vec{F} \parallel \langle 111 \rangle,$$

where $\Delta'_{111} = (d'/\sqrt{3})s_{44}T$. Here b' and d' are the deformation-potential constants of the acceptor ground state for \vec{F} along the $\langle 100 \rangle$ and $\langle 111 \rangle$ directions, respectively,⁷ s_{11} , s_{12} , and s_{44} are the elastic compliance constants, and T is the stress produced by \vec{F} . Here the prime is used to designate quantities associated with the impurity. Since T is defined to be positive for tensile force, the signs of b' and d' are determined by the behavior of a given state. Thus for \vec{F} along either $\langle 100 \rangle$ or $\langle 111 \rangle$, m_J remains a "good quantum number," whereas for a general direction this is not so, the expression for the splitting of the state involving both b' and d' .

Using group-theoretical arguments, the symmetries of the stress-induced sublevels of a given state may be deduced^{9,23} in the usual way. This is shown in Fig. 2 for $\vec{F} \parallel \langle 100 \rangle$ and $\vec{F} \parallel \langle 111 \rangle$. It is seen, for example, that under a $\langle 100 \rangle$ force, \vec{T}_d reduces to \vec{D}_{2d} and, consequently, $\Gamma_8 \rightarrow \Gamma_6 + \Gamma_7$. By use of projection operators, it can be verified that of the four basis functions of the Γ_8 ground state characterized by $J = \frac{3}{2}$, the two for which $m_J = \pm \frac{3}{2}$ form the basis of Γ_6 of \vec{D}_{2d} while Γ_7 belongs to those for which $m_J = \pm \frac{1}{2}$.¹⁷ Thus, the sublevel characterized by $E_{\pm 3/2}$ in Eq. (1) is of Γ_6 symmetry, etc.; similarly for $\vec{F} \parallel \langle 111 \rangle$. Hence, states with Γ_8 symmetry split into two twofold-degenerate states. The levels under stress retain the twofold spin degeneracy as is required by Kramers's theorem; hence the Γ_5 and Γ_6 of \vec{C}_{3v} , for $\vec{F} \parallel \langle 111 \rangle$, are degenerate, and the twofold degeneracy of Γ_6 and Γ_7 of \vec{T}_d is not lifted.

Symmetry arguments also enable selection rules for optical transitions to be deduced.^{9,23} These are shown in Fig. 2 for $\vec{F} \parallel \langle 100 \rangle$ and $\vec{F} \parallel \langle 111 \rangle$, where the electric vector of the light \vec{E} is either parallel or perpendicular to \vec{F} . For $\vec{F} \parallel \langle 110 \rangle$, Γ_6 , Γ_7 , and Γ_8 of \vec{T}_d reduce to Γ_5 , Γ_5 , and $2\Gamma_5$, respectively, of \vec{C}_{2v} . In this case, the selection rules permit all transitions for both polarizations and all directions of \vec{q} , the direction of light propagation, although for the orthorhombic point group C_{2v} a \vec{q} dependence of the intensities for $\vec{E} \perp \vec{F}$ can

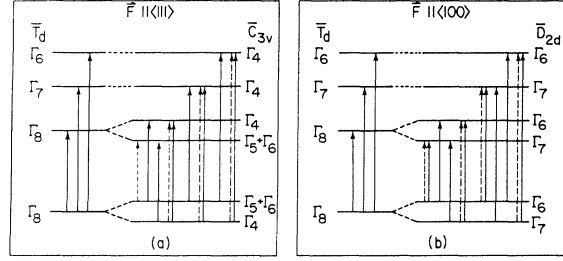


FIG. 2. Behavior of transitions from a Γ_8 ground state to Γ_6 , Γ_7 , and Γ_8 excited states of the double group \vec{T}_d under uniaxial compression. The dashed arrows are for $\vec{E} \parallel \vec{F}$ while the full arrows are for $\vec{E} \perp \vec{F}$.

be expected in general.¹¹ Group-theoretical techniques can be further used to calculate relative intensities of the stress-induced components of a given transition, provided the symmetries of the initial and final states of the components are known. Onton *et al.*¹¹ calculated these intensities following the theoretical treatment of Kaplyanskii.²³ The ratio of two undetermined parameters C_ψ and C_ϕ appears in this calculation for the components of a line arising from a $\Gamma_8 \rightarrow \Gamma_8$ transition, while only one such parameter occurs in the calculation for $\Gamma_8 \rightarrow \Gamma_6$ or $\Gamma_8 \rightarrow \Gamma_7$ transitions. Thus for the latter two cases the relative intensities may be calculated exactly.^{11,23} The components of the $\Gamma_8 \rightarrow \Gamma_6$ transition have relative intensities as 3:1:4, i.e., $(\Gamma_5 + \Gamma_6 \rightarrow \Gamma_4)_\perp : (\Gamma_4 \rightarrow \Gamma_4)_\perp : (\Gamma_4 \rightarrow \Gamma_4)_\parallel$ for $\vec{F} \parallel \langle 111 \rangle$ and $(\Gamma_6 \rightarrow \Gamma_6)_\perp : (\Gamma_7 \rightarrow \Gamma_6)_\perp : (\Gamma_7 \rightarrow \Gamma_6)_\parallel$ for $\vec{F} \parallel \langle 100 \rangle$, where the subscripts \perp and \parallel denote that the electric vector of the radiation is perpendicular and parallel, respectively, to \vec{F} . The intensity ratio of the components of the $\Gamma_8 \rightarrow \Gamma_7$ transition are the same as for the corresponding components of the $\Gamma_8 \rightarrow \Gamma_6$ transition. The relative intensities of the components of the $\Gamma_8 \rightarrow \Gamma_8$ transition for $\vec{F} \parallel \langle 111 \rangle$ and $\vec{F} \parallel \langle 100 \rangle$ are plotted in Fig. 3 as a function of the ratio of the undetermined parameters C_ψ and C_ϕ .¹¹ Dickey and Dimmock¹⁰ have used the wave functions of Mendelson and James⁶ for acceptors in germanium to calculate the relative intensities of some of the stress-induced components of the D line for $\vec{F} \parallel \langle 100 \rangle$, and find that the intensity ratio $(\Gamma_7 \rightarrow \Gamma_6)_\parallel : (\Gamma_7 \rightarrow \Gamma_6)_\perp$ is 2:1 while that of $(\Gamma_6 \rightarrow \Gamma_7)_\perp : (\Gamma_6 \rightarrow \Gamma_7)_\parallel$ is 3:1.²⁴ These values should unambiguously determine the C_ψ/C_ϕ ratio for the D line since, in such a calculation, no undetermined parameters remain. That this is so can be seen from Fig. 3, in which there is only one region for $\vec{F} \parallel \langle 100 \rangle$ at which these ratios are compatible. The value of C_ψ/C_ϕ for the 2:1 ratio lies slightly to the right of -0.2 , while that of the 3:1 ratio lies slightly to the left of -0.2 . These values of C_ψ/C_ϕ are represented by the solid vertical lines shown in Fig. 3. Of course,

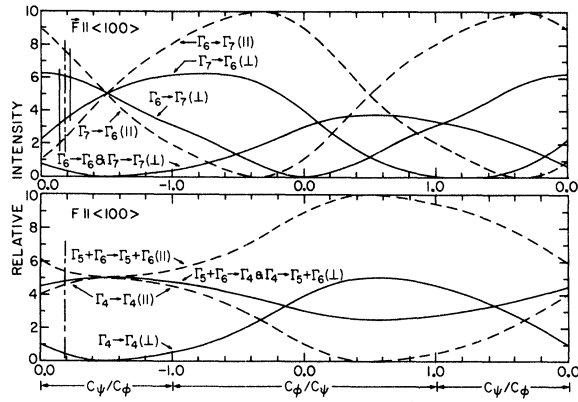


FIG. 3. Relative intensities of stress-induced components of a $\Gamma_8(\bar{T}_d) \rightarrow \Gamma_8(\bar{T}_d)$ transition for stress along $\langle 111 \rangle$ or $\langle 100 \rangle$. The intensities, deduced from symmetry considerations, are plotted as functions of $C_\psi:C_\phi$, where these are the two arbitrary constants demanded in this case (see Ref. 11). The two vertical lines for $\bar{F} \parallel \langle 100 \rangle$ represent the values of C_ψ/C_ϕ determined from Dickey and Dimmock's (Ref. 10) intensity calculations for the D line of group-III acceptors in germanium. The vertical dot-dash lines at $C_\psi/C_\phi = -0.2$ represent the mean of these two values.

only one value of C_ψ/C_ϕ should hold for a given $\Gamma_8 \rightarrow \Gamma_8$ transition. The fact that two slightly different values are obtained may be due to two possibilities: Firstly, Mendelson and James's envelope functions for the various states are not purely s -like and p -like, whereas the results plotted in Fig. 3 have been calculated using basis functions of just one type for each state¹¹; and secondly, the ratios given by Dickey and Dimmock may have been "rounded off." It is interesting to note that a relatively unambiguous value of C_ψ/C_ϕ results from these two independent calculations. The vertical dot-dash lines in Fig. 3 represent the mean value of the two solid vertical lines. The value of C_ψ/C_ϕ for a given line is dependent on the unperturbed states, and hence will be the same for all directions of stress. Thus, the value of $C_\psi/C_\phi \approx -0.2$ deduced for the D line from Dickey and Dimmock's intensity ratios for $\bar{F} \parallel \langle 100 \rangle$ will also be applicable to the D line for $\bar{F} \parallel \langle 111 \rangle$, as implied in Fig. 3. It should be pointed out that the results presented in Fig. 3 apply to two equally populated ground-state sublevels, i. e., they are valid in the limiting case of zero ground-state splitting.

In the case of $\bar{F} \parallel \langle 110 \rangle$, the intensities are a function of the ratio $\Delta'_{111}/\Delta'_{100}$. The behavior of the intensity of the components for a $\Gamma_8 \rightarrow \Gamma_6$ (or Γ_7) transition as a function of this ratio has been given by Kaplyanskii²³ and plotted by Onton,²⁵ and Onton *et al.*¹¹ The relative intensities of the tran-

sition between the sublevels of two Γ_8 states depend on the ratio C_ψ/C_ϕ and the splitting-parameter ratio $\Delta'_{111}/\Delta'_{100}$ for the ground state and a corresponding one for the excited state. Without reliable values for these splitting parameters, it is not meaningful to attempt a detailed comparison with experiment for this case.

Similar expressions to those of Eqs. (1) and (2) hold for the valence-band edge except that the deformation-potential constants are different.^{21,22} For the valence band the two constants with which we are concerned have been designated by Pikus and Bir as b and d . From Schechter's⁵ ground-state wave functions of acceptors in germanium, Bir *et al.*⁷ have obtained the relationships

$$b' = 0.56b, \quad d' = 0.61d. \quad (3)$$

Identical ratios have also been obtained by Suzuki *et al.*⁸ using their own effective-mass wave functions for the ground state.

IV. EXPERIMENTAL RESULTS

The excitation spectrum of thallium impurity in germanium is shown in Fig. 4.¹² The behavior of this spectrum under uniaxial compression has been studied with the applied force along $\langle 100 \rangle$, $\langle 111 \rangle$, or $\langle 110 \rangle$. The spectra have been examined with light polarized either parallel or perpendicular to \bar{F} . The former will be designated by E_{\parallel} and the latter by E_{\perp} , where E refers to the electric vector of the radiation. In the spectra to be described, the curves for E_{\parallel} will be shown dashed while those for E_{\perp} will be solid. The zero-stress positions of the lines will be indicated by a circled label and an associated vertical arrow.

The effect of compression on the spectrum of thallium for $\bar{F} \parallel \langle 100 \rangle$ is shown in Figs. 5-7. In Fig. 5, it is seen that the C line has split into at least two strong components with well-defined polarizations. There is a distinct asymmetry on the low-energy side of the perpendicular component which suggests that the low-energy component, dominant for E_{\parallel} , may also be present for E_{\perp} . The D line has not split, but does show distinct dichroism. This is also the case for the B and A lines. The G line has not been studied. In both Figs. 6 and 7, the C line is split further and gives rise to four well-defined components labeled $C_1, C_2, C_3,$ and C_4 ; the first two of these are prominent for E_{\parallel} , while the other two, C_3 and C_4 , are prominent for E_{\perp} . The D line splits into the components $D_1, D_2, D_3,$ and D_4 . In Figs. 6 and 7, D_2 and D_3 are well resolved and occur for both E_{\parallel} and E_{\perp} . For E_{\perp} , component D_4 is clearly seen in Fig. 6 and is also present in Fig. 7, while the only indication of D_1 is in the latter figure. For the largest-stress case, Fig. 7, a well-defined high-

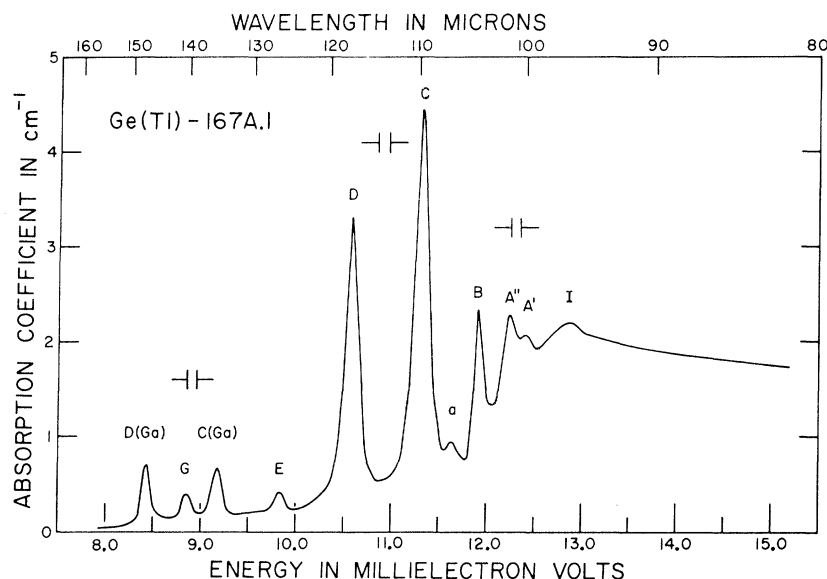


FIG. 4. Excitation spectrum of thallium impurity in germanium; N_A (acceptor concentration) $\cong 3 \times 10^{14} \text{ cm}^{-3}$. Liquid helium used as coolant. The lines designated by C(Ga) and D(Ga) are believed to be due to gallium contamination (see Ref. 12).

energy B component B_2 is seen for both E_{\parallel} and E_{\perp} .

In the measurements of Dickey and Dimmock,¹⁰ the spectra for gallium and indium impurities under a $\langle 100 \rangle$ compression are very similar to those presented here for thallium. These authors have also observed the effect of $\vec{F} \parallel \langle 100 \rangle$ on the spectrum of thallium impurity, but without polarized light. It is not clear why the intensities of the C

components in this case are so weak relative to those of the D components (see Fig. 6, Ref. 10). This is not so for the other impurities studied by them, indium and gallium, and is also quite different from the present results for thallium.

The present measurements for $\vec{F} \parallel \langle 100 \rangle$ are summarized in Fig. 8. The meaning of the vertical arrow in this figure will be discussed later. The energies of the stress-induced components are plotted as a function of the separation of the D_2 and D_3 components. The data of Fig. 5 are not included in this summary since the resolution was not sufficient to separate D_2 from D_3 . In the measurement for which $D_3 - D_2$ is 0.13 meV, it should be mentioned that the C_3 component was stronger than the C_4 component, contrary to the data at larger stress shown in Figs. 6 and 7. This spec-

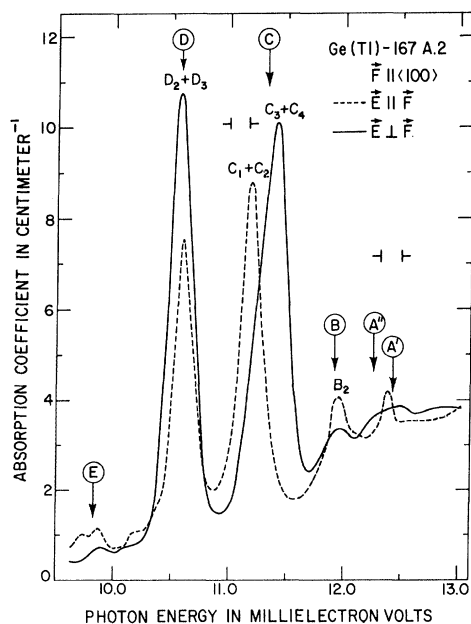


FIG. 5. Excitation spectrum of thallium impurity in germanium under a $\langle 100 \rangle$ compressive force; $N_A \cong 3 \times 10^{14} \text{ cm}^{-3}$. The vertical arrows with circled labels indicate the energies of the zero-stress lines.

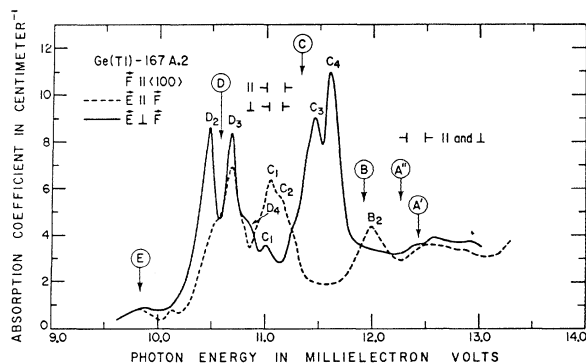


FIG. 6. Excitation spectrum of thallium impurity in germanium under a $\langle 100 \rangle$ compressive force; $N_A \cong 3 \times 10^{14} \text{ cm}^{-3}$. Liquid helium used as coolant. The vertical arrows with circled labels indicate the energies of the zero-stress lines.

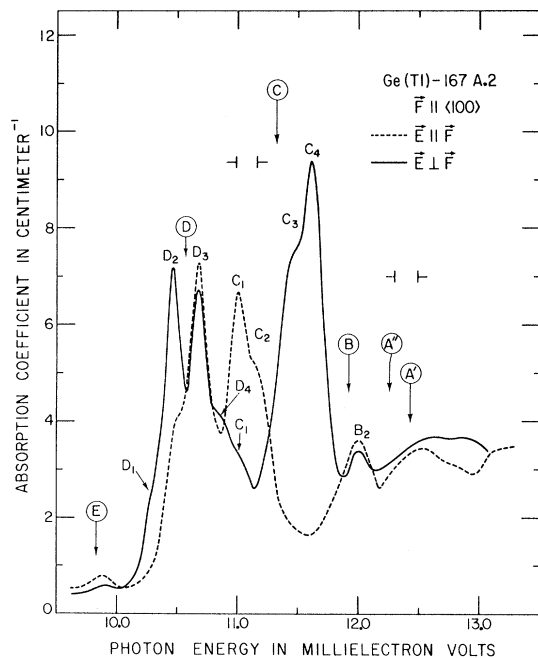


FIG. 7. Excitation spectrum of thallium impurity in germanium under a $\langle 100 \rangle$ compressive force; $N_A \approx 3 \times 10^{14} \text{ cm}^{-3}$. Liquid helium used as coolant. The vertical arrows with circled labels indicate the energies of the zero-stress lines.

trum is not presented since the measurement was not complete; it is for this reason that the position of the B_2 component is not included in Fig. 8.

The behavior of the spectrum of thallium for $\vec{F} \parallel \langle 111 \rangle$ is shown in Fig. 9. The labeling of the stress-induced components will be discussed later. The D line splits into two components, each of which occurs for both E_{\parallel} and E_{\perp} , and are nearly symmetrically disposed about the zero-stress position. The behavior of the C line is almost the same as that of the D line, except that the low-energy C component appears to be present only for E_{\perp} . A low-energy B component B_1 has been observed by Dickey and Dimmock.¹⁰ For the measurement shown in Fig. 9, B_1 should occur at about the same position as C_2 . The effect of compression along $[110]$ for $\vec{q} \parallel [1\bar{1}0]$ is shown in Fig. 10. The horizontal arrows indicate the manner in which the various components behave under larger stress. This behavior was deduced from the results of another measurement for which the stress was slightly higher than that of Fig. 10. The stress-induced components have not been labeled in this case.

V. DISCUSSION

Previous interpretations of the behavior of the excitation spectra of the group-III impurities under

uniaxial compression^{9,10} have been based on the assumption that the B line of the spectrum is due to the transition $(8+0) \rightarrow (7-1)$, i. e., a transition between a fourfold-degenerate Γ_8 ground state and a twofold-degenerate Γ_7 excited state. This assumption was suggested by the correlation given in Fig. 1, and appeared to be justified by the observation that only one B component occurred for E_{\parallel} with $\vec{F} \parallel \langle 100 \rangle$, while the relative intensities of the observed components were in agreement with the predictions.¹⁰ Accepting this interpretation, this transition immediately gives the orderings and the splittings of the ground-state sublevels, and hence the signs and magnitudes of the deformation-potential constants for the ground state.

In the present case, for $\vec{F} \parallel \langle 100 \rangle$, the selection rules of Fig. 2 for a $\Gamma_8 \rightarrow \Gamma_7$ transition applied to the B line demonstrate that Γ_6 would be the lower ground-state sublevel. Of course, the interpretation of the behavior of the remaining lines must be consistent with this choice of ground-state ordering. In the case of the D line this was apparently so while some success was achieved in understanding the C line if its final state consisted of the two levels depicted in Fig. 1. For $\vec{F} \parallel \langle 100 \rangle$, the component D_2 was deduced to be the transition $\Gamma_6 \rightarrow \Gamma_7$

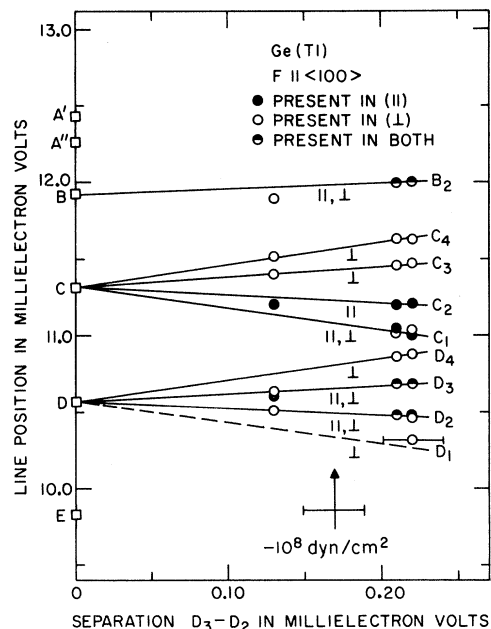


FIG. 8. Energies of the stress-induced components of the B , C , and D excitation lines of thallium impurity in germanium under $\langle 100 \rangle$ compression as a function of the separation between components D_3^{\perp} and D_2^{\perp} . The dashed line labeled D_1 has been drawn such that separation $D_3 - D_1$ equals $D_4 - D_2$. The vertical arrow calibrates the abscissa in terms of stress. This has been accomplished by the use of Fig. 6 of Ref. 10.

rather than $\Gamma_7 \rightarrow \Gamma_6$, since the predicted relative intensities are $(\Gamma_6 \rightarrow \Gamma_7)_\perp > (\Gamma_6 \rightarrow \Gamma_7)_\parallel$ (see Fig. 3) and $(\Gamma_7 \rightarrow \Gamma_6)_\perp < (\Gamma_7 \rightarrow \Gamma_6)_\parallel$; in which case, D_2 is the $\Gamma_7 \rightarrow \Gamma_6$ transition and should exhibit the intensity ratio $D_3^{\parallel} : D_3^{\perp} :: 2:1$, in qualitative agreement²⁶ with the experimental observation, except in the case of Fig. 6. Further, the magnitude of the splittings of the ground state as predicted by the B line can be reconciled with the energy spacings of the D components. The theory correctly predicts that the components D_1^{\perp} and D_4^{\perp} should be very weak. Thus, the behavior of the D line, to a considerable extent, is consistent with the previous interpretation of the origin of the B line. However, when comparison of the calculated and observed intensities of the D components is continued, a direct contradiction arises. From Fig. 3, it is predicted that the intensity ratio $D_3^{\perp} : D_2^{\perp} = (\Gamma_7 \rightarrow \Gamma_6)_\perp : (\Gamma_6 \rightarrow \Gamma_7)_\perp :: 3:5$; thus, since the upper ground-state sublevel will become depopulated relative to the lower, experimentally the intensity of D_3^{\perp} should be less than $0.6D_2^{\perp}$. This is certainly not so and constitutes a serious contradiction.

The above interpretation for $\vec{F} \parallel \langle 100 \rangle$ leads to several other difficulties. Firstly, since it re-

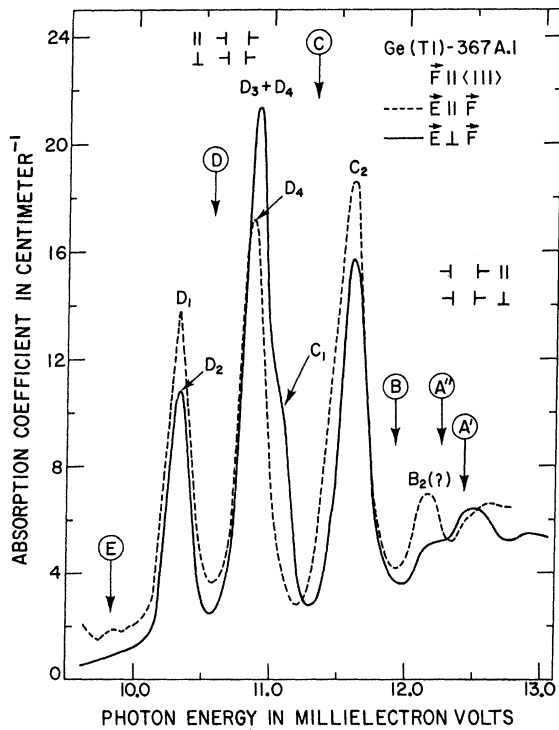


FIG. 9. Excitation spectrum of thallium impurity in germanium under a $\langle 111 \rangle$ compression; $N_A \approx 5 \times 10^{14} \text{ cm}^{-3}$. Liquid helium used as coolant. The vertical arrows with circled labels indicate the energies of the zero-stress lines.

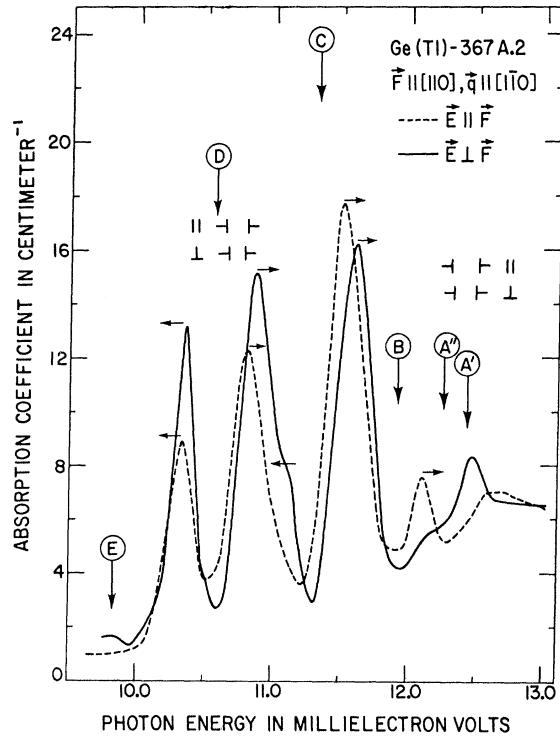


FIG. 10. Excitation spectrum of thallium impurity in germanium with the compressive force parallel to $[110]$ and $\vec{q} \parallel [1\bar{1}0]$, where \vec{q} is the direction of light propagation; $N_A \approx 5 \times 10^{14} \text{ cm}^{-3}$. Liquid helium used as coolant. Motion of the components for a slight increase in stress is indicated by the horizontal arrows. The vertical arrows with circled labels indicate the energies of the zero-stress lines.

quires that the Γ_6 sublevel of the ground state moves to lower hole energy under compression, $E_{\pm 3/2}$ of Eq. (1) is negative. Hence, since $s_{11} - s_{12}$ is positive,²⁷ both b' and b are positive in contradiction to the negative sign obtained for b by other methods.²⁸⁻³¹ Secondly, the magnitude of b so obtained is significantly different from that otherwise determined. Thirdly, the ground-state ordering is opposite to that deduced for group-III impurities in silicon,¹¹ contrary to that which might be expected.

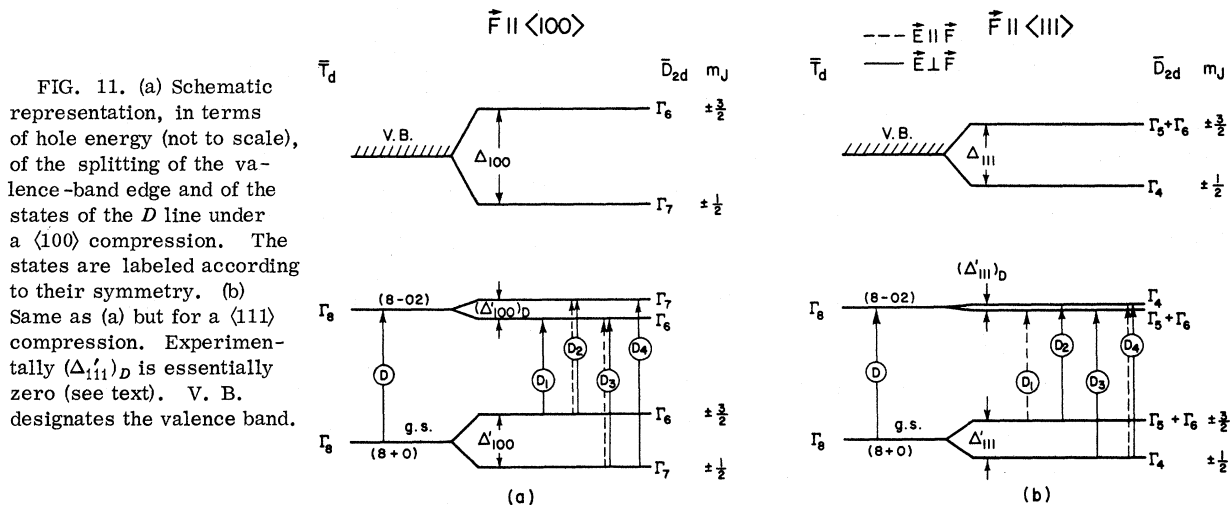
An interpretation has also been given previously¹⁰ for the effect of a $\langle 111 \rangle$ compression on the group-III spectra in germanium. In this case, too, the sign and magnitude of the corresponding deformation-potential constant d of the valence band deduced^{10,32} from Eq. (3) are different from those obtained by other methods.²⁸⁻³¹

The above interpretation pivots on the assumption that the final state of the B line has Γ_7 symmetry. It should be pointed out that the position of the (8-12) state has not been calculated, al-

though Dickey and Dimmock have tentatively assigned this to the final state of the A'' line. However, if the sequence of energies of the $3p$ -like states is the same as that of the $2p$ -like states, viz., $\Gamma_8, \Gamma_8, \Gamma_7, \Gamma_6$, one would expect the (8-12) state to lie between the (8-11) and the (7-1) states. Thus, it is possible that the (8-12) state is the final state of the B line rather than the (7-1) state. There is, in fact, some experimental evidence that the B line does not have a Γ_7 final state. It has been shown by Dickey and Dimmock that the component B'_1 , present for E_{\parallel} (see Fig. 14, Ref. 10)³³ has its origin in the B line. Thus, since only one parallel B component is allowed with Γ_7 as the final state (see Figs. 2 and 3), Dickey and Dimmock have suggested that the parallel component at ~ 10.6 meV is a low-energy A'' component. Similar remarks hold for the case of gallium impurity (see Fig. 15, Ref. 10). They have not been able to follow the high-energy parallel component as a function of stress; however, if their interpretation is correct, this component should move to lower energies with increasing stress. This does not appear to be the case, as may be seen from Fig. 9, which corresponds to a stress about twice as large³⁴ as that of either Fig. 11 or 14 of Ref. 10. In fact, the position of the parallel component at 12.17 meV in Fig. 9 is consistent with the stress-dependence curve given by Dickey and Dimmock for the B'_2 component of indium impurity.

In view of the above ambiguity regarding the nature of the B transition, the behavior of the D line will be used to determine the effect of stress on the ground state. The D line is chosen in preference to the C line because of the complexity of the final state of the latter. In what follows, all previous conclusions based on the origin of the B line will be discarded.

For $\vec{F}_{\parallel} \langle 100 \rangle$, the number of stress-induced components observed for the D line and their polarization is clearly that predicted for a $\Gamma_8 \rightarrow \Gamma_6$ transition. The fact that for E_{\parallel} the two intermediate components D_2 and D_3 are observed, reduces the number of possible arrangements of the four stress-induced substates involved from eight to four. These four arrangements depend upon which ground-state sublevel is the lower and whether the ground state splits more or less than the excited state. It is possible to eliminate the two cases which correspond to D_2 being the $\Gamma_7 \rightarrow \Gamma_6$ transition. As pointed out earlier, the population-independent intensity ratio $(\Gamma_7 \rightarrow \Gamma_6)_{\parallel} : (\Gamma_7 \rightarrow \Gamma_6)_{\perp}$ for the D line is calculated to be 2:1, while experimentally, D_2^{\parallel} is of much smaller intensity than D_2^{\perp} ; hence D_2 must correspond to the transition $\Gamma_6 \rightarrow \Gamma_7$, and D_3 to the transition $\Gamma_7 \rightarrow \Gamma_6$. Thus, the intensity ratio $D_3^{\parallel} : D_3^{\perp}$ should be 2:1. Experimentally, it is found that the parallel component of D_3 has a larger peak intensity than does the perpendicular component.²⁶ In view of the difficulties encountered experimentally in obtaining a well-resolved spectrum, it is not possible to give a quantitative estimate of this ratio. It is also calculated that the ratio $(\Gamma_6 \rightarrow \Gamma_7)_{\parallel} : (\Gamma_6 \rightarrow \Gamma_7)_{\perp}$ is 3:1 independent of the population of the ground states. Thus, the components D_2^{\perp} and D_3^{\parallel} should have intensities in this ratio, in qualitative agreement with experiment. It is thus seen that the above assignments for the transitions giving rise to the components D_2 and D_3 are in general agreement with experiment. The remaining two cases still depend upon which of the two ground-state sublevels is the lower and whether $(\Delta'_{100})_D \geq \Delta'_{100}$, where $(\Delta'_{100})_D$ is the splitting of the excited state of the D line. In order to differentiate these two cases, it is necessary to consider the intensity ratios of transitions from different ground-state



sublevels. The relative intensities of these will be dependent upon the relative populations of the two ground-state sublevels as pointed out earlier. A comparison will be made between only those components which have the same polarization; thus ambiguity due to the different resolution attained for the two directions of polarization will be avoided. The intensity ratio $(\Gamma_7 \rightarrow \Gamma_6)_I : (\Gamma_6 \rightarrow \Gamma_7)_I$ is about 3:5, while that of $(\Gamma_7 \rightarrow \Gamma_6)_\parallel : (\Gamma_6 \rightarrow \Gamma_7)_\parallel$ is 3:1. If Γ_7 is the upper ground state, then in view of the depopulation effects, the intensity of D_3^I should be less than 0.6 times that of D_2^I ; experimentally, this ratio is almost 1. Similarly, the intensity of D_3^\parallel should be less than three times that of D_2^\parallel ; experimentally, D_3^\parallel is considerably larger than D_2^\parallel . If Γ_7 is the lower ground state, the intensity of D_3^I should be larger than 0.6 times that of D_2^I while D_3^\parallel should have an intensity which is more than three times that of D_2^\parallel . Clearly, the experimental intensity ratio $D_3^I : D_2^I$ being greater than 0.6 is sufficient to show that the lower ground state is Γ_7 . The fact that the intensity of D_3^\parallel is much larger than that of D_2^\parallel supports this conclusion but is not sufficient to unambiguously differentiate the two cases. With this choice of lower ground state, it is necessary that $\Delta'_{100} > (\Delta'_{100})_D$ as shown in Fig. 11(a). From this it is also seen that the splitting of the ground state is determined by the spacing of either D_1 and D_3 , or D_2 and D_4 .³⁵ In the quantitative-stress measurements of Dickey and Dimmock, the components D_1 and D_4 were not observed and hence the ground-state splitting, in their case, cannot be determined from the D components. However, the spacing D_3 to D_2 in their spectrum for thallium under a $\langle 100 \rangle$ compression (see Fig. 6, Ref. 10) can be used to calibrate the stress for the present measurements in which the ground-state splitting has been determined. It is estimated that the D_3 to D_2 separation for thallium corresponds to $(1.7 \pm 0.2) \times 10^{-9}$ meV/dyn cm⁻². This value has been used to locate the vertical arrow corresponding to a compression of 10^8 dyn/cm² shown in Fig. 8. The values obtained for the deformation-potential constants b' and b using this stress gauge and the splitting $D_4 - D_2$ are given in Tables I and II, respectively. This value of b is consistent in both sign and magnitude with the values obtained by other methods²⁸⁻³¹ (see Table II). The sign of b is, of course, opposite to that obtained by Dickey and Dimmock since the present ordering of the sublevels of the ground state is opposite to that obtained previously.

The $\langle 100 \rangle$ data for the C line, summarized in Fig. 8, show that within experimental error, the spacings $C_4 - C_2$ and $C_3 - C_1$ are the same as that of $D_4 - D_2$, the ground-state splitting. Thus, using the spacing $C_4 - C_2$ as the ground-state splitting,

TABLE I. Deformation-potential constants of group-III impurities in germanium.

Impurity	b' (eV) ^a	d' (eV) ^b	d'/b'	b'/b_D^c
Ga	-1.15 ± 0.16	-2.2 ± 0.4	$+1.9 \pm 0.5$	-2.2 ± 0.7
In	-1.4 ± 0.2	-2.9 ± 0.4	$+2.2 \pm 0.6$	-1.9 ± 0.4
Tl	-1.5 ± 0.2	-2.1 ± 0.6
	-1.3 ± 0.4^d			

^aObtained from the splittings $C_5 - C_3$ of Figs. 6-8 of Ref. 10.

^bObtained from the D components of Figs. 15 and 16 of Ref. 10.

^c b_D^c is defined to be the deformation-potential constant of the excited state of the D line for $\bar{F} \parallel \langle 100 \rangle$. The ratios b'/b_D^c have been obtained from Figs. 8 and 10 of Ref. 10 and Fig. 6 of the present measurements. The negative sign is a consequence of the opposite ordering of the ground-state sublevels relative to those of the excited state [see Fig. 11(a)].

^dObtained using the splitting $D_4 - D_2$ of the data of Fig. 6, employing Fig. 6 of Ref. 10 to gauge the stress.

the data of Dickey and Dimmock for the C components³⁶ can also be used to obtain b' . For thallium, using Fig. 6 of Ref. 10, the values so obtained for b' and b are given in Tables I and II, respectively. In this manner, b' and b have also been obtained for gallium and indium impurities, and are also included in Tables I and II.

A reinterpretation of the data for the C components for $\bar{F} \parallel \langle 100 \rangle$, assuming this to be a $\Gamma_8 \rightarrow \Gamma_7 + \Gamma_8$ transition, reduces the number of choices of energy schemes to the two shown in Figs. 12(a) and 12(b) and have been obtained in the following way. In Sec. IV, it was mentioned that at small stress the component C_3 was stronger than component C_4 . Since this is not the case for larger stresses it implies that the intensity of C_3 increases relative to that of C_4 as the stress decreases, implying that C_4 originates from the lower ground-state sublevel whereas C_3 arises from the upper.³⁷ Also, the spacing between C_3 and C_4 is less than Δ'_{100} . Thus, the final state of C_3 must lie above that of C_4 by an amount less than Δ'_{100} . Further, as discussed above, the spacing $C_4 - C_2$ measures Δ'_{100} . If C_2 had arisen from the lower ground state, viz., Γ_7 , then its final state would lie Δ'_{100} below that of C_4 and have Γ_6 symmetry, since C_2 is observed for E_\parallel . However, with this interpretation, the selection rules and energy spacings would not allow a parallel C component whose energy is smaller than that of C_2 . Hence, C_2 would appear to originate from the upper ground state and have the same final state as C_4 . The symmetry of this latter state must then be Γ_7 . The two cases given in Fig. 12 arise from the two possible choices for the initial state of the C_1 com-

TABLE II. Deformation-potential constants of the valence band of germanium by various methods.^a

Deformation-potential constant	Piezospectroscopic study of group-III acceptors				Other techniques			
	Present interpretation ^b			Dickey and Dimmock ^c	Γ^d	Π^e	III^f	IV^g
	Ga	In	Tl					
b	-2.0 ± 0.2	-2.4 ± 0.4	-2.6 ± 1.4	$+0.9 \pm 0.1$	-2.1 ± 0.2	$ 2.7 \pm 0.3 $	-2.4 ± 0.2	-2.6 ± 0.2
d	-3.6 ± 0.7	-4.8 ± 0.7	...	$+2.1 \pm 0.2$	-7.0 ± 1.5	$ 4.7 \pm 0.5 $	-4.1 ± 0.4	-4.7 ± 0.3

^aUnits are eV.^bCalculated from the values given for b' and d' in Table I using the expressions of Eq. (3).^cThese values are quoted in Ref. 10. However, if the interpretation used by these authors is followed, from their published data for Ga and In it is estimated that $d = +4.7$ eV. The origin of the quoted value of $+2.1$ is not clear (see Ref. 32).^dPiezo studies of acceptor binding energies from Hall measurements (see Ref. 28).^ePiezospectroscopy of the direct exciton (see Ref. 29).^fPiezoreflectance of the direct absorption edge (see Ref. 30).^gPiezolectroreflectance of the direct absorption edge (see Ref. 31).

ponent. In both cases, the position of the final state of this component has been determined from the observation that $C_3 - C_1 \approx \Delta'_{100}$. The selection rules determine the symmetry of the final state of C_1 . In the case of Fig. 12(b), it should be noted that the splitting of the ground state and the extreme sublevels of the excited state are the same. Hence, for this case C_3 may consist of not only the transition $(\Gamma_6 \rightarrow \Gamma_6)_L$, but also the transition

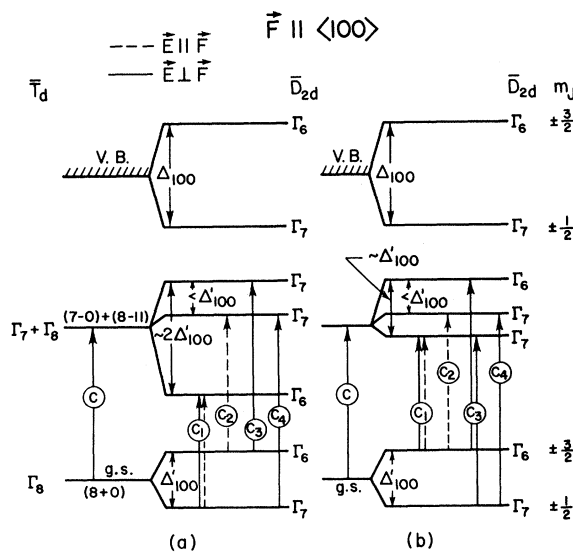


FIG. 12. Schematic representation, in terms of hole energy (not to scale), of the behavior of the states of the C line under a $\langle 100 \rangle$ compression. The two diagrams (a) and (b) are the two proposals which best fit the experimental observations assuming that the final state of the C line is the combination $\Gamma_7 + \Gamma_8$. V. B. designates the valence band.

$(\Gamma_7 \rightarrow \Gamma_7)_L$. There is some experimental evidence that favors the case of Fig. 12(a) in that, for the measurement at $D_3 - D_2 = 0.13$ meV of Fig. 8, the peak energy of the unresolved parallel C_1 and C_2 components occurs at about the predicted mean energy of these components. This implies that as the stress decreases the intensity of the C_2 component increases relative to that of C_1 , suggesting that C_1 has the lower ground state as initial state. However, the present experimental evidence is not sufficient to unambiguously differentiate these two cases, nor is it sufficient to justify any attempt to determine the interaction between the two final Γ_7 substates involved. No comparison can be made between the experimental and predicted intensities of the C components without a detailed knowledge of this interaction, except for transitions to the noninteracting Γ_6 state. Hence, for Fig. 12(a), the experimental intensity ratio of $C_1^{\parallel} : C_1^{\perp}$ should correspond to some value of C_{ψ} / C_{ϕ} in Fig. 3. From Figs. 6 and 7, it is seen that $C_1^{\parallel} \gg C_1^{\perp}$. This inequality can be accommodated at either $C_{\psi} / C_{\phi} \approx +0.8$ or $C_{\psi} / C_{\phi} \approx +0.2$. For Fig. 12(b) the transitions $(\Gamma_7 \rightarrow \Gamma_6)_{\parallel}$ and $(\Gamma_7 \rightarrow \Gamma_6)_L$ are not observed, even though they should be enhanced by population effects. The closest approach to this situation is at $C_{\psi} / C_{\phi} \approx +0.2$. However, even for this choice the predicted intensities appear to be too large for the lines not to have been observed. Hence, this consideration tends again to favor Fig. 12(a). In both Figs. 12(a) and 12(b), the spacing $C_4 - C_2$ is a direct measure of Δ'_{100} , consistent with the use of this spacing to obtain values of b' for all the impurities.

In order to reinterpret the effect of a $\langle 111 \rangle$ compression, the behavior of the D line will again

be considered. For this case, it is predicted that two parallel and three perpendicular components should be observed and the component $\Gamma_4 \rightarrow \Gamma_4$, common to both directions of polarization, should be weak for E_1 at $C_\psi/C_\phi \approx -0.2$ (see Fig. 3). This is consistent with the observation of two relatively strong parallel components and two relatively strong perpendicular components. From the selection rules shown in Fig. 2, it is clear that the difference in energy between a given parallel component and either one or the other of the two strong perpendicular components measures either the ground-state splitting or the excited-state splitting. Hence, as may be seen from Fig. 9, either Δ'_{111} or $(\Delta'_{111})_D$, the splitting of the excited state, is very small. The results and conclusions obtained¹⁰ for gallium and indium impurity are essentially the same as this, except that it is not clear why the two components D'_3 and D'_4 of Fig. 14, Ref. 10³³ do not have the same energy since D'_1 and D'_2 do coincide.

If the ground state undergoes very little splitting, then the spectrum will exhibit virtually no depopulation effects and the deformation-potential constant d' will be essentially zero.³⁸ If depopulation effects occur then it is the excited state which is unsplit. From the selection rules, it is seen that the two parallel components have different ground-state sublevels as initial states. From Figs. 14 and 15 of Ref. 10 for indium and gallium, and Fig. 9 of the present results for thallium, it is seen that as the spacing $D_4 - D_1$ increases so does the intensity of the high-energy parallel D component relative to that of the low-energy parallel component.³⁹ Such an effect is also observed for the perpendicular components and is particularly noticeable when a comparison is made between the spectra of Fig. 14 of Ref. 10 and Fig. 9. Thus it is concluded that there are depopulation effects and that the splitting of the D components is entirely due to the splitting of the ground state.

It now remains to order the sublevels of the ground state. This can be done by a comparison of the calculated intensities with those observed. From Fig. 3, for $C_\psi/C_\phi \approx -0.2$, it is estimated that the intensity ratios are,⁴⁰ independent of depopulation effects,

$$(a) (\Gamma_{5+6} \rightarrow \Gamma_{5+6})_{\parallel} / (\Gamma_{5+6} \rightarrow \Gamma_4)_1 \approx 1.1 ,$$

$$(b) [(\Gamma_4 \rightarrow \Gamma_4) + (\Gamma_4 \rightarrow \Gamma_{5+6})]_{\perp} / (\Gamma_4 \rightarrow \Gamma_4)_{\parallel} \approx 1.1 ;$$

and, for equal population of ground-state sublevels,

$$(c) (\Gamma_4 \rightarrow \Gamma_4)_{\parallel} / (\Gamma_{5+6} \rightarrow \Gamma_{5+6})_{\parallel} \approx 0.9 ,$$

$$(d) [(\Gamma_4 \rightarrow \Gamma_4) + (\Gamma_4 \rightarrow \Gamma_{5+6})]_{\perp} / (\Gamma_{5+6} \rightarrow \Gamma_4)_1 \approx 1.1 .$$

If the lower sublevel of the ground state is Γ_4 as

shown in Fig. 11(b),⁴¹ then with the labeling given, which is also the labeling used in Fig. 9, the predicted intensity ratios become, independent of depopulation effects,

$$(a) D_1^{\parallel} / D_2^{\perp} \approx 1.1 ,$$

$$(b) (D_4 + D_3)^{\perp} / D_4^{\parallel} \approx 1.1 ;$$

and, including expected depopulation effects,

$$(c) D_4^{\parallel} / D_1^{\parallel} > 0.9 ,$$

$$(d) (D_4 + D_3)^{\perp} / D_2^{\perp} > 1.1 .$$

Experimentally, $D_1^{\parallel} / D_2^{\perp} \approx 1$ and $(D_4 + D_3)^{\perp} / D_4^{\parallel} > 1$ for all measurements, while $D_4^{\parallel} / D_1^{\parallel} > 1$ for Fig. 9 but is a little less than 1 for Figs. 14 and 15 of Ref. 10. The experimental ratio $(D_4 + D_3)^{\perp} / D_2^{\perp} > 1$ for Fig. 15, Ref. 10, and Fig. 9, but is slightly less than 1 for Fig. 14, Ref. 10. These estimates are based on peak intensity without any attempt to take into account background absorption or linewidth.

If Γ_4 is the upper sublevel of the ground state and the same ordering of the excited state is retained, then the predicted intensity ratios would be,⁴² independent of depopulation effects,

$$(a) D_3^{\parallel} / D_4^{\perp} \approx 1.1 ,$$

$$(b) (D_2 + D_1)^{\perp} / D_2^{\parallel} \approx 1.1 ,$$

and, including expected depopulation effects,

$$(c) D_2^{\parallel} / D_3^{\parallel} < 0.9 ,$$

$$(d) (D_2 + D_1)^{\perp} / D_4^{\perp} < 1.1 .$$

Experimentally, $D_3^{\parallel} / D_4^{\perp} < 1$ and $(D_2 + D_1)^{\perp} / D_2^{\parallel} \sim 1$ for all cases, while $D_2^{\parallel} / D_3^{\parallel} > 1$ for Figs. 14 and 15 of Ref. 10, and < 1 for Fig. 9. The experimental ratio $(D_2 + D_1)^{\perp} / D_4^{\perp} < 1$ for Fig. 15 of Ref. 10 and Fig. 9, and ~ 1 for Fig. 14 of Ref. 10.

From the above it is seen that neither case agrees unambiguously with the predictions. However, the ground-state ordering represented in Fig. 11(b) is clearly to be preferred, since only one serious violation occurs for this case; the ordering so obtained is again opposite to that deduced by Dickey and Dimmock.¹⁰ From the quantitative data of these authors, values of d' and d have been estimated for both gallium and indium. These are included in Tables I and II. The magnitude of Δ'_{111} in each case has been gauged from the energy difference between the high- and low-energy D components.

A satisfactory reinterpretation of the stress behavior of the C line for $F_{\parallel} \langle 111 \rangle$ has not yet been made.¹⁷ If it is assumed that the final state of the C line is a $\Gamma_7 + \Gamma_8$, predicted by Mendelson and James,⁶ the experimental facts are sufficient to reduce the number of possible energy schemes to

four. None of these cases is completely consistent with the intensity predictions. However, it is not clear to what extent these predictions are affected by possible interaction between the two stress-induced Γ_4 substates which are part of the decomposition of the excited state.

The splitting of a fourfold-degenerate state for $\bar{F}_{\parallel}\langle 110\rangle$ is determined by the values of the deformation-potential constants for $\bar{F}_{\parallel}\langle 111\rangle$ and $\bar{F}_{\parallel}\langle 100\rangle$. Thus, the results obtained for $\bar{F}_{\parallel}\langle 110\rangle$ can be used to verify the conclusions arrived at for the other two directions of compression. It has been shown^{7,23} that the splitting of the ground state for $\bar{F}_{\parallel}\langle 110\rangle$ is given by

$$\Delta'_{110} = [(b')^2(s_{11} - s_{12})^2 + \frac{1}{4}(d')^2 s_{44}^2]^{1/2} T, \quad (4)$$

with similar expressions for the excited Γ_8 states. Hence, with a knowledge of the various deformation-potential constants the value of the ratio $\Delta'_{110}/(\Delta'_{110})_D$ can be predicted. In this way, it is possible, in principle, to differentiate between the various interpretations of the data. In both the present interpretation and that of Dickey and Dimmock,¹⁰ the value of d'_D is zero, where d'_D is defined as the deformation-potential constant for $\bar{F}_{\parallel}\langle 111\rangle$ of the excited state involved in the D transition. In this case, inserting the experimental values²⁷ for the elastic constants into Eq. (4) gives

$$\left| \frac{\Delta'_{110}}{(\Delta'_{110})_D} \right| = \left| \frac{b'}{b'_D} \right| \left[1 + 0.36 \left(\frac{d'}{b'} \right)^2 \right]^{1/2}. \quad (5)$$

In the interpretation of Dickey and Dimmock,¹⁰ the values of b'/b'_D and d'/b' for indium impurity are 0.45 ± 0.07 and 2.8 ± 0.5 , respectively. These ratios lead to a value of 0.9 ± 0.2 for $\Delta'_{110}/(\Delta'_{110})_D$. Using the same interpretation, but the value of $d' = 2.8 \pm 0.3$ eV³² obtained by reevaluating Dickey and Dimmock's data, a value of 1.6 ± 0.5 was obtained for the ratio of Eq. (5). The values of b'/b'_D and d'/b' listed in Table I, i.e., those obtained using the present interpretation, give a value of 3.2 ± 1.2 . It is found (see Tables 2 and 4 of Ref. 10 and Table I) that the ratios of deformation-potential constants appearing in Eq. (5) are essentially species independent; hence the above three different values of $\Delta'_{110}/(\Delta'_{110})_D$ for indium impurity can be used to predict the pattern of the components of the D line for thallium impurity. The only value of $\Delta'_{110}/(\Delta'_{110})_D$ which is at all compatible with the data of Fig. 10 is that obtained using the present interpretation. In the other two cases, either three or four well-separated D components should be observed. Dickey and Dimmock have used their values of b' and d' to predict the splitting of the B line for $\bar{F}_{\parallel}\langle 110\rangle$ and state that

they have obtained agreement with their experimental value. However, from the above, it is apparent that their data for the D line should not agree with their interpretation. Unfortunately, their spectra for $\bar{F}_{\parallel}\langle 110\rangle$ were not presented and hence this point cannot be verified.

From Eq. (4), a result similar to that of Eq. (5) can be obtained for the case where $d' = 0$, a possibility which was rejected in the discussion of $\bar{F}_{\parallel}\langle 111\rangle$. In this case, the ratio $|\Delta'_{110}/(\Delta'_{110})_D|$ is found to be 0.7 ± 0.2 , a value incompatible with the pattern for the D components of Fig. 10. This further justifies rejection of this case.

VI. CONCLUSION

It has been seen that if the stress-induced splitting of the ground state of a group-III acceptor in germanium is deduced from the behavior of the D line, then the deformation-potential constants of the valence band obtained from those of the impurity ground state are in agreement both in sign and magnitude with values found by other methods. The conclusion that both the ground state and the final state of the D line have Γ_8 symmetry is in agreement with theory. The deductions regarding the final state of the C line are not as clear as those for the D line. The data do show that the C line has a complex final state, but it has not been verified unambiguously that this is the $\Gamma_7 + \Gamma_8$ combination predicted by theory, nor has the spacing between these two states been determined. However, a recent study of singly ionized zinc in germanium⁴³ suggests that this spacing is ~ 0.04 meV. The success in interpreting the behavior of the ground state from that of the D line implies that the symmetry of the final state of the B line is not Γ_7 . It is suggested that it is the (8-12) state, a level not calculated by Menselson and James,⁶ or else a combination of this with some other states.

It should be remarked here that the orderings of the ground-state sublevels deduced from the D line for both $\bar{F}_{\parallel}\langle 100\rangle$ and $\bar{F}_{\parallel}\langle 111\rangle$ are the same as those obtained in a similar study of four of the group-III impurities in silicon.^{11,25} In addition, the relative intensities of the components of the D line of group-III impurities in germanium are quite similar to those of the components of line 2 of boron, aluminum, and indium in silicon, in that for $\bar{F}_{\parallel}\langle 100\rangle$ there are strong central components flanked by very weak components, even though the ratio of ground- to excited-state splitting is not the same for these two transitions. Also, for these two excitations, the ordering of the stress-induced sublevels of the excited states is the same. For the case of singly ionized zinc in germanium,⁴³ the behavior of the D line is almost identical to that of line 2 of boron impurity in silicon. It

would appear, then, as if the $\Gamma_8 - \Gamma_8$ transition giving rise to the D line of single acceptors in germanium is of the same type as that of line 2 for group-III acceptors in silicon. A study of the G line of such acceptors in germanium would presumably reveal the similarity of this transition with that of line 1 of acceptors in silicon.

There is some indication that the constants b' and d' have a slight species dependence. These appear to become larger, the larger the chemical shift of the ground state of the impurity,¹² presumably owing to slight differences in the wave functions for this state and thus the relations of Eq. (3), calculated using the effective-mass wave functions, should not be expected to be exact.

However, ignoring these differences, the average values of b' and d' are -1.4 and -2.5 eV, respectively, which lead in turn to the values of -2.5 and -4.1 eV, for b and d .

ACKNOWLEDGMENTS

The authors wish to thank Professor A. K. Ramdas for many valuable discussions and for a critical reading of the manuscript. They also thank Professor S. Rodriguez for a valuable discussion. They are indebted to Miss Louise Roth for ingots and orienting the samples and to Professor H. J. Yearian also for orienting some of the samples.

¹Work supported in part by the Advanced Research Projects Agency and the National Science Foundation.

*Present address: Ohio State Research Foundation at Aerospace Research Laboratories, Wright-Patterson AFB, Ohio 45433.

¹P. J. Price, Phys. Rev. **104**, 1223 (1956).

²D. K. Wilson and G. Feher, Phys. Rev. **124**, 1068 (1961).

³P. Fisher and A. K. Ramdas, in *Physics of the Solid State*, edited by S. Balakrishna, M. Krishnamurthi, and B. Ramachandra Rao (Academic, New York, 1969), p. 149.

⁴W. Kohn, in *Solid State Physics*, Vol. 5, edited by F. Seitz and D. Turnbull (Academic, New York, 1957), p. 257.

⁵D. Schechter, J. Phys. Chem. Solids **23**, 237 (1962).

⁶K. S. Mendelson and H. M. James, J. Phys. Chem. Solids **25**, 729 (1964).

⁷G. L. Bir, E. I. Butikov, and G. E. Pikus, J. Phys. Chem. Solids **24**, 1467 (1963).

⁸K. Suzuki, M. Okazaki, and H. Hasegawa, J. Phys. Soc. Japan **19**, 930 (1964).

⁹R. L. Jones and P. Fisher, Solid State Commun. **2**, 369 (1964).

¹⁰D. H. Dickey and J. O. Dimmock, J. Phys. Chem. Solids **28**, 529 (1967). Note that the classification of p -envelope functions under \bar{O}_h given on p. 532 of this reference should be Γ_4^- not Γ_5^- .

¹¹A. Onton, P. Fisher, and A. K. Ramdas, Phys. Rev. **163**, 686 (1967).

¹²R. L. Jones and P. Fisher, J. Phys. Chem. Solids **26**, 1125 (1965).

¹³R. D. Hancock and S. Edelman, Rev. Sci. Instr. **27**, 1082 (1956); see also J. W. Edwards, Semicond. Prod. **6**, 30 (1963); **6**, 34 (1963).

¹⁴H. M. Randall, D. M. Dennison, N. Ginsbury, and L. R. Weber, Phys. Rev. **52**, 160 (1937); L. R. Blaine, E. K. Plyler, and W. S. Benedict, J. Res. Natl. Bur. Std. A **66**, 223 (1962); K. Narahari Rao, R. V. deVore, and E. K. Plyler, *ibid.* **67**, 351 (1963).

¹⁵P. Fisher, W. H. Haak, E. J. Johnson, and A. K. Ramdas, in *Proceedings of the Eighth Symposium on the Art of Glassblowing* (American Scientific Glass-

blowing Society, Wilmington, Del., 1963), p. 136.

¹⁶A. C. Rose-Innes, Proc. Phys. Soc. (London) **72**, 514 (1958).

¹⁷R. L. Jones, Ph. D. thesis, Purdue University, 1968 (unpublished).

¹⁸J. H. Reuszer and P. Fisher, Phys. Rev. **140**, A245 (1965).

¹⁹A. Mitsuishi, Y. Yamada, S. Fujita, and H. Yoshinaga, J. Opt. Soc. Am. **50**, 433 (1960).

²⁰The notation used is that of G. F. Koster, J. O. Dimmock, R. G. Wheeler, and H. Statz, *Properties of the Thirty-Two Point Groups* (MIT Press, Cambridge, Mass., 1965).

²¹G. E. Pikus and G. L. Bir, Fiz. Tverd. Tela **1**, 1642 (1959) [Soviet Phys. Solid State **1**, 1502 (1959)].

²²W. H. Kleiner and L. M. Roth, Phys. Rev. Letters **2**, 334 (1959).

²³A. A. Kaplyanskii, Opt. i Spektroskopiya **16**, 1031 (1964) [Opt. Spectry. (USSR) **16**, 557 (1964)].

²⁴These ratios have been obtained from Table 1 and Fig. 3 of Ref. 10 with the correlation that $\Delta_i(\bar{D}_{2d}) = \Gamma_i(\bar{D}_{2d})$, where $i=6, 7$.

²⁵A. Onton, Ph. D. thesis, Purdue University, 1967 (unpublished).

²⁶This is so for Fig. 7 of this paper and for Figs. 7 and 8 of Ref. 10; it is not so for Fig. 6. However, in this latter measurement, the spectral slit width for E_1 was smaller than that for E_{11} , and hence the peak intensities of components for E_1 will be exaggerated compared to those for E_{11} .

²⁷H. B. Huntington, in *Solid State Physics*, Vol. 7, edited by F. Seitz and D. Turnbull (Academic, New York, 1958), p. 213.

²⁸J. J. Hall, Phys. Rev. **128**, 68 (1962).

²⁹A. M. Glass, Can. J. Phys. **43**, 12 (1965).

³⁰I. Balslev, Solid State Commun. **5**, 315 (1967).

³¹F. H. Pollack and M. Cardona, Phys. Rev. **172**, 816 (1968).

³²Using Dickey and Dimmock's published data and the splitting of the B line to measure Δ_{111}' for indium impurity, a value of $d = +4.6 \pm 0.5$ eV is obtained. It is not clear why this value is so different from that of $+2.1 \pm 0.2$ eV quoted by these authors.

³³Note that in this reference the various stress-induced

components for $\vec{F} \parallel \langle 111 \rangle$ are designated by a prime.

³⁴The magnitude of the stress for Fig. 9 has been gauged from the splitting coefficient of the D line as deduced from Dickey and Dimmock's data for indium impurity. This assumes that d' is about the same for both indium and thallium.

³⁵The dashed line in Fig. 8 has been drawn such that the spacings D_4-D_2 and D_3-D_1 are equal. Clearly the shoulder designated as D_1 in Fig. 7 fits this quite well.

³⁶The spacing C_4-C_2 is used rather than C_3-C_1 since in the interpretation given later C_4-C_2 is a direct measure of the ground-state splitting whereas C_3-C_1 is not. Note that the labeling of the C components in Ref. 10 is different from that used here. In addition, it would appear that the component designated C_4 in Fig. 6 of Ref. 10 is mislabeled since the spacing C_4-C_2 in that figure is not the same as C_5-C_3 , whereas the latter is (within experimental error) the same as that predicted from the data of Fig. 8. However, the small feature at ~ 11.6 meV in Fig. 6 of Ref. 10 is the same energy difference from C_2 as C_5 is from C_3 and, hence, could be the C_4 component.

³⁷This conclusion has been reached by assuming that any stress dependence of the wave functions, expected in principle for the perturbed $\Gamma_7 + \Gamma_8$ final state, has a much smaller effect on the relative intensities than do the depopulation effects caused by the splitting of the ground state.

³⁸If this were the case, clearly there would be little meaning to Eq. (3).

³⁹It should be pointed out that here we are comparing the intensities of stress-induced spectra which arise from different group-III impurities. However, the relative intensities of the zero-stress lines vary very little from one group-III impurity to another (see Ref. 12), indicating that the ground-state wave functions vary only slightly from one impurity to another. Hence the C_6/C_6' ratio for a given transition should be relatively species independent. This appears to be substantiated by the case of group-III acceptors in silicon, in which quite a large change occurs in the ratio of deformation-potential constants of the ground and excited states of line 2 in going from boron and aluminum to indium; yet the relative intensities of the stress-induced compounds of this line are little affected.

⁴⁰Note that $\Gamma_{5+6} \equiv \Gamma_5 + \Gamma_6$.

⁴¹In this figure, the excited state is shown as split. This has been done for convenience in labeling the transitions, the order chosen for these substates being arbitrary since they are not separated experimentally.

⁴²It should be noted that with this order for the ground-state sublevels, a given transition will bear a different label since the observed components of a line have been numbered starting at the lowest-energy component. In this case, which is not the case for which Fig. 9 is labeled, D_1^I , D_2^I , D_2^{II} , D_3^{II} , and D_4^I occur and not D_1^{II} , D_3^I , and D_4^{II} .

⁴³F. Barra and P. Fisher, Phys. Letters 27A, 711 (1968).